© 2000 Oxford University Press
Human Molecular Genetics, 2000, Vol. 9, No. 4 645–651

Mutation of the receptor tyrosine kinase gene *Mertk* in the retinal dystrophic RCS rat

Patricia M. D'Cruz, Douglas Yasumura[1], Jessica Weir, Michael T. Matthes[1], Hadi Abderrahim[+], Matthew M. LaVail[1] and Douglas Vollrath[§]

Department of Genetics, Stanford University School of Medicine, Stanford, CA 94305-5120, USA and [1]Departments of Anatomy and Ophthalmology, University of California, San Francisco School of Medicine, San Francisco, CA 94143-0730, USA

Received 17 November 1999; Revised and Accepted 23 December 1999 DDBJ/EMBL/GenBank accession nos AF208235 and AF208236

Vertebrate photoreceptor cells are the basic sensory apparatus of the retina, capable of converting the energy of absorbed photons into neuronal signals. The proximal portions of mammalian photoreceptor outer segments are synthesized daily by cell bodies, and outer segment tips are shed with a circadian rhythm, resulting in a complete turnover of outer segments about every 9 days. The shed outer segments are phagocytosed by adjacent retinal pigment epithelial (RPE) cells, and metabolites are recycled to photoreceptors. The Royal College of Surgeons (RCS) rat is a widely studied, classic model of recessively inherited retinal degeneration in which the RPE fails to phagocytose shed outer segments, and photoreceptor cells subsequently die. We have used a positional cloning approach to study the *rdy* (retinal dystrophy) locus of the RCS rat. Within a 0.3 cM genetic inclusion interval, we have discovered a small deletion of RCS DNA that disrupts the gene encoding the receptor tyrosine kinase Mertk. The deletion includes the splice acceptor site upstream of the second coding exon of *Mertk* and results in a shortened transcript that lacks this exon. The aberrant transcript joins the first and third coding exons, leading to a frameshift and a translation termination signal 20 codons after the AUG. The concordance of these and other data indicate that *Mertk* is probably the gene for *rdy*. Our results provide genetic evidence for an essential role of a receptor tyrosine kinase in a specialized form of phagocytosis and suggest a molecular model for ingestion of outer segments by RPE cells.

INTRODUCTION

Proper functioning of the basic sensory apparatus of the mammalian retina depends on the cooperation of two distinct cell types, the photoreceptor cell and the retinal pigment epithial (RPE) cell, which are intimately associated in the outer retina. The continual synthesis and shedding of photoreceptor outer segments places a substantial biosynthetic load on the photoreceptor cell. Part of the function of the RPE cell is to lighten this burden, through phagocytosis of shed outer segments and recycling of retinoids and membrane lipids to the photoreceptor cell (1,2). The Royal College of Surgeons (RCS) rat is an animal model of recessively inherited retinal degeneration in which the process of cooperation between the photoreceptor cell and the RPE has gone awry, resulting in a progressive, postnatal loss of photoreceptor cells (3,4). Histological examination of the RCS retina reveals an abnormal build-up of outer segment debris between the photoreceptor cell outer segment layer and the RPE that occurs prior to and concomitant with photoreceptor cell death (5–8). Genetic chimera (9) and RPE cell transplantation (10) experiments have localized the defect in the RCS rat to the neuroectoderm-derived RPE cells, and RCS RPE cells fail to phagocytose isolated outer segments in culture (11).

One hypothesis regarding the nature of the RCS RPE phagocytosis defect is that ingestion may require binding of a specific receptor on the RPE to a ligand on the outer segment (12), and that RCS RPE cells lack functional receptors. Indeed, normal rat RPE cells show a degree of specificity for ingestion of outer segments *in vitro* when offered a variety of particles (13). The phagocytosis defect is not general because RCS RPE cells or explants can ingest latex beads and carbon particles (11,14) and RCS peritoneal phagocytes display normal function in culture (15). Candidate receptors that have been proposed include $\alpha_v\beta_5$ integrin (16), mannose receptor (17) and CD36 (18), but none of these proteins has been shown conclusively to be defective in the RCS rat. Recently, extensive genetic and genomic resources for the laboratory rat have become widely available (19–23), facilitating work on this important model organism. We therefore decided to take a positional cloning approach to identification of the retinal dystrophy locus (*rdy*) with the aim of gaining insight into the normal and abnormal interactions between the RPE and photoreceptor cells, and into the molecular mechanisms of outer segment ingestion by the RPE cells.

[+]Present address: Genset Genomic Research Center, RN 7, 91030 Evry cedex, France
[§]To whom correspondence should be addressed. Tel: +1 650 723 3290; Fax: +1 650 723 7016; Email: vollrath@genome.stanford.edu

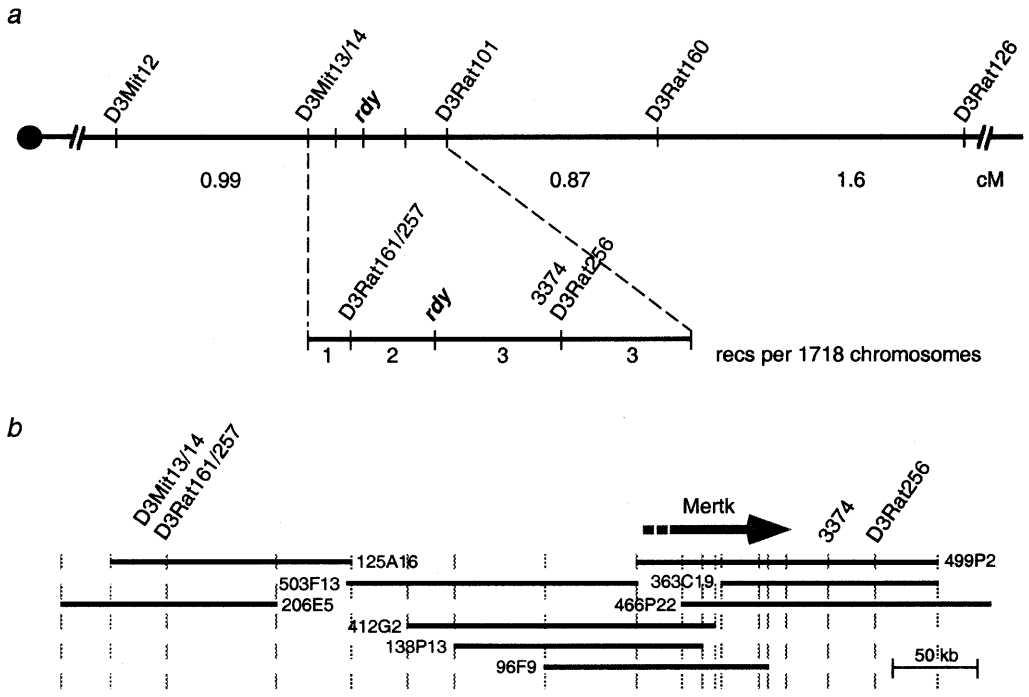

Figure 1. Genetic and physical maps of the *rdy* region. (**a**) A total of 1718 N_2 progeny from an RCS × BN backcross were genotyped with *D3Mit12* and *D3Rat126*, which bracket *rdy*. Recombinant chromosomes were scored with additional markers within the interval and genotypes at *rdy* were inferred by retinal histology. Genetic distance in cM or the number of recombinants between adjacent markers is shown. (**b**) Physical map of the *rdy* genetic inclusion interval. Shown are selected BAC clones (horizontal black lines) and sequence-tagged sites (STSs; vertical dashed lines) within the inclusion interval between *D3Rat161/257* and marker 3374, and which are part of a much larger BAC/STS content map. Most STSs derive from BAC insert ends. This, in combination with insert size information, provides an estimate of the extent of insert overlap and the distances between STSs (28). The *Mertk* gene is located to one side of the interval, and all of the coding exons fall within BAC 499P2, although the precise location of the first coding exon was not determined. No other genes were detected in the inclusion interval.

RESULTS

Genetic mapping of *rdy*

Rudimentary genetic mapping previously had localized *rdy* ~19 cM from *nonagouti* and 32 cM from *Svp-1* on rat chromosome 3 (24). To confirm this localization, we scored 30 microsatellite markers from distal chromosome 3 (25) on DNA from RCS and a congenic strain RCS-*rdy*$^+$ (26) into which a wild-type *rdy* allele from the Fischer 344 strain had been introgressed. RCS alleles were observed for most markers, but markers *D3Mgh11* and *D3Mit12* displayed an F344 allele in the congenic strain, indicating retention of a block of F344 DNA through selection for the wild-type *rdy* allele.

To locate *rdy* precisely, we constructed a high resolution genetic map of the region. DNA genotyping and retinal histology were performed for an initial group of progeny from an RCS × F344 backcross, and the locus was localized to an ~15 cM interval between markers *D3Mit4* and *D3Rat104*. Animals with recombination breakpoints within this interval were scored with additional markers, and *rdy* was confined to a 4–5 cM subinterval bounded by markers *D3Mit12* and *D3Rat126*. The backcross was expanded to 1455 N_2 progeny, all of which were genotyped with *D3Mit12* and *D3Rat126*, and retinal histology was performed on 70 animals with recombination breakpoints in the interval to infer genotypes at *rdy*. During the course of this work, eight additional markers appeared on public genetic maps of the region (Whitehead Institute/MIT Center for Genome Research, Rat Genomic Mapping Project, Data Release 6, November, 1998: http://waldo.wi.mit.edu/rat/public/), but none of these were polymorphic between RCS and F344. However, seven of the eight markers were polymorphic between RCS and the Brown Norway (BN) rat, which appears to be a genetic outlier with respect to other inbred rat strains (27).

We initiated a second backcross between RCS and BN. Combined genotyping and retinal histology on an initial group of 110 N_2 progeny showed that the retinal dystrophic phenotype segregated as expected and appeared very similar to that observed in the F344 cross. Genotypes were determined at *D3Mit12* and *D3Rat126* for a total of 1718 N_2 progeny, and retinal histology was obtained for 69 animals with recombination breakpoints within the interval. These recombinants were scored with seven additional markers to create a high resolution genetic map of the region and confine *rdy* to an inclusion interval of ~0.3 cM and bracketed by *D3Rat161*/*D3Rat257* and *D3Rat256* (Fig. 1a).

Construction of physical maps of the *rdy* region

Our efforts to construct a genetic map of the *rdy* region were aided by simultaneous construction of physical maps because the higher resolution of the physical maps and lack of a requirement for polymorphism allowed us to order markers that were unresolved on genetic maps. Yeast artificial chromosome (YAC) clones were isolated by screening a library with *D3Rat101*, which initially was non-recombinant with *rdy*, and sequence-tagged sites (STSs) were generated from clone ends. Because chimeric clones are common in most YAC libraries, we used radiation hybrids to determine whether end STSs mapped to the region of interest.

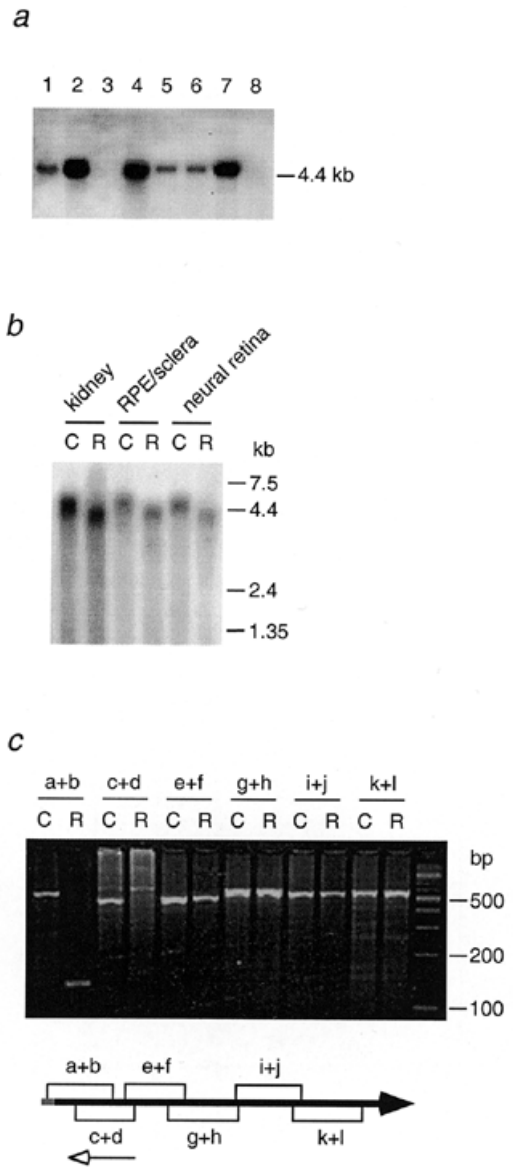

Figure 2. Expression of rat *Mertk* mRNA. (**a**) An antisense DNA probe from near the 5′ end of the rat *Mertk* cDNA was hybridized to a multiple tissue northern blot (Clontech) containing the following samples: 1, testis; 2, kidney; 3, skeletal muscle; 4, liver; 5, lung; 6, spleen; 7, brain; 8, heart. Hybridization with an actin control probe showed that the heart RNA is under-represented. The position of a 4.4 kb size standard is indicated. (**b**) Comparison of *Mertk* transcripts between dystrophic RCS (R) and normal congenic (C) RCS-*rdy*$^+$ animals. A total of 2.5 μg of poly(A)-selected mRNA was loaded for each sample and hybridized with the probe used in (a) after membrane transfer. The positions of RNA size standards are indicated. (**c**) RT–PCR analysis of *Mertk* transcripts in RPE/scleral RNA from RCS and congenic RCS-*rdy*$^+$. The ~3 kb *Mertk* coding region (black arrow) is drawn to scale below the gel image with the cDNA segments amplified by various primer combinations indicated, along with the location of an antisense probe (open arrow) used in (a) and (b). All primer pairs used (Table 1) amplified across splice junctions in the cDNA.

Isolation of additional YACs with YAC end STSs and *D3Rat161*, *D3Rat257* and *D3Rat256* resulted in a redundant contig that extended from markers *D3Mit13/Mit14* to *D3Rat101* (data not shown).

We began isolating bacterial artificial chromosome (BAC) clones across the interval covered by the YAC contig because BACs are largely free of the cloning artifacts found in YACs. As the genetic mapping progressed, our efforts focused on the interval between *D3Rat161/Rat257* and *D3Rat256*. We constructed a highly redundant BAC contig spanning this interval and beyond by simultaneous walking from multiple entry points (28). A new polymorphic microsatellite marker (3374) was generated from a BAC end sequence and used to narrow further the genetic inclusion interval, which is more than covered by three minimally overlapping BAC clones (Fig. 1b).

Routine BLAST analysis of sequences near insert ends revealed two with a high degree of similarity to different parts of a murine *Mertk* cDNA sequence. The order of the two end sequences indicated that the orientation of transcription of the gene is from centromere to telomere. Placement on the BAC contig of an STS developed with oligonucleotide primers from the 3′-untranslated region (3′-UTR) of murine *Mertk*, and sequencing from BAC clone 499P2 with primers from the beginning of the open reading frame, demonstrated that the entire coding portion of the gene lies within the *rdy* genetic inclusion interval (Fig. 1b).

Sequence and expression analysis of *Mertk* in normal and dystrophic rats

Mertk encodes a receptor tyrosine kinase expressed in monocytes, epithelia and reproductive tissues (29) that is a member of a family of at least three receptor tyrosine kinases, which also includes Axl and Tyro3, with ectodomains composed of two immunoglobulin and two fibronectin domains, similar to neural cell adhesion molecules (30). The prior association of *Mertk* with adhesion, epithelia and phagocytic monocytes, along with location of the gene within the genetic inclusion interval, made it an attractive *rdy* candidate.

We used oligonucleotide primers designed from partial rat sequence and murine *Mertk* cDNA sequence to amplify overlapping segments covering the entire coding region of rat *Mertk* by RT–PCR. Sequencing of RT–PCR products revealed that the rat gene encodes a 994 amino acid protein and shares 91.8% nucleotide identity and 91.5% amino acid identity with murine *Mertk*, suggesting that the two genes are orthologous.

We assessed expression of rat *Mertk* in normal and dystrophic animals by northern analysis and RT–PCR (Fig. 2). The expression profile in normal, outbred Sprague–Dawley rats (Fig. 2a) is similar to that in mice (31). Comparison of RPE/sclera, neural retina and kidney mRNA samples from RCS and RCS-*rdy*$^+$ strains revealed a slightly smaller transcript in dystrophic animals (Fig. 2b). RT–PCR analysis was consistent with the northern results. Overlapping segments spanning most of the coding region could be amplified from both RCS and RCS-*rdy*$^+$ samples, but primer pairs from the 5′ end of the coding region either amplified a smaller segment (Fig. 2c, primers a + b) or failed to amplify sequences (Fig. 2c, primers c + d) from RCS cDNA, indicating a deletion of 5′ sequences from the RCS *Mertk* transcript.

Mutation of *Mertk* in RCS rats

We determined the genomic structure of the 5′ coding region of rat *Mertk* by sequence walking on DNA from clone 499P2 (Fig. 3). Comparison of the genomic structure with the sequence of the a + b RT–PCR product from RCS cDNA (Fig. 2c) revealed a precise deletion in the aberrant transcript of 409 bases,

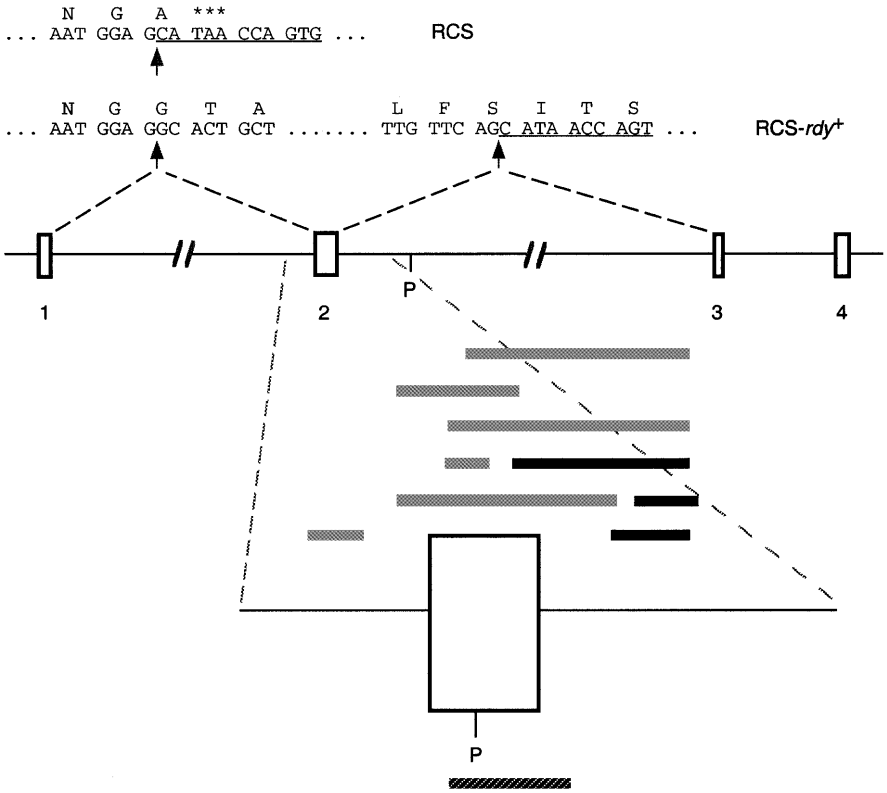

Figure 3. Structure of *Mertk* 5′ genomic and cDNA sequences in normal and dystrophic rats. The genomic structure of the first four coding exons and adjoining introns of wild-type *Mertk* is depicted in the middle. Partial cDNA sequences from the 5′ end of *Mertk*, obtained from RCS and RCS-*rdy*$^+$ animals, are shown above, with the locations of splice junctions indicated by arrows. Sequence at the beginning of the third coding exon is underlined, and a premature translation termination signal in the RCS transcript is indicated by three asterisks. A depiction of PCR results obtained by amplifying segments in and around the second coding exon (GenBank accession no. AF208236) is shown below. Gray horizontal bars indicate products amplified from RCS-*rdy*$^+$ DNA that could not be amplified from RCS DNA. Black bars indicate products that were obtained from both DNAs. The lower portion of the figure is drawn to scale. The hatched bar at the bottom denotes the location of a hybridization probe used for Southern analysis of restriction digested RCS and RCS-*rdy*$^+$ DNA. P, *Pst*I site.

corresponding to the second coding exon. Conceptual translation of the deleted mRNA shows a frameshift after codon 19, followed almost immediately by a translation termination codon (Fig. 3).

PCR analysis of RCS and RCS-*rdy*$^+$ genomic DNA demonstrated that, although the 3′ half of exon 2 and adjoining intron sequences could be amplified from both strains, primers from the 5′ half of exon 2 or upstream intron sequences failed to yield a product from RCS DNA (Fig. 3), indicating a deletion of sequences from the RCS genome. Southern analysis of RCS and RCS-*rdy*$^+$ genomic DNA digested with one of nine different restriction enzymes and probed with a segment from the second coding exon (the location of which is shown in Fig. 3) revealed that the restriction fragment detected in RCS DNA was usually 1.5–2 kb smaller than that detected in RCS-*rdy*$^+$ DNA, with the exception of fragments generated by *Pst*I digestion, where the RCS fragment was ~8 kb larger than the RCS-*rdy*$^+$ fragment (data not shown). The 5′ end of the smaller, wild-type *Pst*I fragment is located within the second coding exon. A deletion of RCS DNA that includes the *Pst*I site in the second coding exon and extends 1.5–2 kb into adjoining 5′ intron sequences is consistent with the Southern hybridization and genomic PCR data.

Together, the structures of the RCS *Mertk* transcript and genomic DNA indicate that a small deletion, which includes the splice acceptor site next to the second coding exon, has resulted in expression of an aberrant transcript that lacks this exon and that is incapable of encoding a functional protein.

The *Mertk* mutation is non-recombinant with *rdy*

We used the presence or absence of a c+d amplification product as a genetic marker to score spleen RNA samples from the five RCS × BN backcross progeny with recombination events closest to *rdy* (Fig. 1a), and found that the *Mertk* RT–PCR marker was non-recombinant with the *rdy* mutation. We also used the presence or absence of a PCR product from the 5′ portion of the second coding exon to score the genomic DNA of all recombinants within the *D3Mit12* and *D3Rat126* interval detected in both the RCS × BN and the RCS × F344 backcrosses. The deletion is non-recombinant with *rdy* in both crosses, a total of 3173 meiotic events.

DISCUSSION

The concordance of the location of *Mertk* within a narrow genetic inclusion interval, a mutated *Mertk* transcript that cannot encode a functional protein, a rearrangement of RCS DNA that explains the aberrant transcript and is non-recombinant with *rdy* in >3000 meioses, and expression of *Mertk* in the RPE/sclera strongly suggests that *Mertk* is the gene disrupted by the *rdy* mutation.

Other, less likely scenarios are also possible, such as the existence of a second mutant gene in the inclusion interval that alone is responsible for the phenotype, or deleterious effects by the deletion on a second gene near to *Mertk*. Functional complementation of the RCS defect by wild-type *Mertk* would rule out these alternatives conclusively.

A mouse strain homozygous for a targeted mutation of *Mertk* that destroys tyrosine kinase activity by removing a single exon near the 3′ end of the coding region exhibits splenomegaly and an increased sensitivity to endotoxins (32). The retinas of the mutant mice apparently were not examined, so a retinal defect may have passed unnoticed. Alternatively, it would not be surprising if the mutant mouse and RCS rat expressed different retinal phenotypes because the mutant murine Mertk protein was intended to have residual function (32). Moreover, a similar mutant Axl receptor with a missense mutation that ablates tyrosine kinase activity can still promote cell adhesion in culture (33). Regardless of which explanation is correct, our results highlight the utility of a phenotype-driven approach to understanding gene function.

A molecular model for phagocytosis of outer segments by RPE

The identification of *Mertk* as the likely *rdy* gene provides insight into the RCS retinal dystrophic phenotype and the mechanism of phagocytosis of outer segments by the RPE cells. Cell culture studies implicate $\alpha_v\beta_5$ integrin, a vitronectin receptor which is present at the RPE–outer segment interface (34), in the binding but not internalization of outer segments by RPE cells (16). It is plausible that Mertk cooperates with $\alpha_v\beta_5$ to phagocytose outer segments and signal the event within RPE cells. Signaling through other receptor tyrosine kinases can promote cell growth (35) or cell migration (36) in a vitronectin receptor-dependent manner, and there are mechanistic similarities between cell migration and phagocytosis (37).

Mertk signaling of phagocytosis may also be important for trophic support of photoreceptors by the RPE. Transplantation of normal RPE cells to the retinas of RCS rats slows degeneration of photoreceptor cells over an area larger than the transplant site (38), and targeted mutation of *Mertk*, *Tyro3* and *Axl* in mice apparently leads to decreased trophic support for developing sperm and other cells, and results in postnatal degeneration of rods and cones in the retina (39).

Gas6, a secreted vitamin K-dependent protein expressed in a variety of tissues, including the retina (D. Vollrath and M.M. LaVail, unpublished data), is a ligand for all three Mer-family receptors (40,41). Gas6 can bind to the outside of cells and promote heterotypic intercellular adhesion through the Axl receptor (33), supporting a role for Mertk and Gas6 in adhesion of the RPE to photoreceptor outer segments. Gas6 preferentially binds to phosphatidylserine (42), an abundant constituent of photoreceptor membranes (43). Phosphatidylserine is present predominantly in the inner membrane leaflet, but is exposed to the exterior of apoptotic cells and oxidized red blood cells (44). Binding of Gas6 to photoreceptor membranes that display phosphatidylserine may provide a mechanism for selective phagocytosis of older outer segments by the RPE.

Relevance to human disease

Mutations responsible for a number of forms of early-onset retinal degeneration in humans have been identified, including mutations associated with Leber congenital amaurosis and retinitis pigmentosa. A large number of other human retinal degeneration loci have been mapped, but mutations have not been described. Human *MERTK* has been mapped to chromosome 2q14.1 (45). To our knowledge, no retinal degeneration locus has yet been linked to this region, but the extensive genetic heterogeneity of the condition in humans and the simple loss-of-function nature of the mutation we have characterized leave open the possibility that mutations in *MERTK* are responsible for a fraction of human early-onset retinal degeneration. Although most genes linked to retinal degeneration are expressed in photoreceptors, a growing minority of genes are expressed in the RPE cells (46–49). The RPE cells are thought to be relevant to the pathogenesis of a common late-onset form of human retinal degeneration, age-related macular degeneration (AMD), because abnormal deposits of lipofuscin-like material known as drusen accumulate in and around the RPE cells in this condition. Given the RPE cell-autonomous nature of the RCS phagocytosis defect and the importance of outer segment renewal to the well being of the photoreceptor cell, it is possible that MERTK, or a molecule with which it interacts, is involved in the pathogenesis of AMD.

MATERIALS AND METHODS

Genetic mapping

DNA for genotyping was isolated from rat spleens by a modification of a previously described protocol (50). A total of 1718 N_2 progeny from a BN × RCS backcross were scored with *D3Mit12* and *D3Rat126* by resolving amplification products on agarose gels stained with ethidium bromide, and recombinants subsequently were scored with additional markers, some of which were labeled with ^{32}P and resolved on sequencing gels (Fig. 1a). A polymorphic CA repeat (3374) was amplified with oligonucleotide primers (CTGGCCTCCATTTGTGTG; TTGAGCAGGAGGCAGAGA) and *Taq* Gold (PE Biosystems, Foster City, CA) by a touchdown PCR protocol. An ~7–10 bp size difference between the BN allele and the smaller RCS allele was detected by agarose gel electrophoresis.

Retinal histology

To infer genotype at *rdy*, P21–P35 backcross progeny were euthanized with carbon dioxide, eyes were immediately enucleated, fixed in a mixture of formaldehyde and glutaraldehyde, bisected along the vertical meridian and embedded in a mixture of Epon–Araldite. Sections of 1 µm of the entire retina were cut and stained with toluidine blue as described elsewhere (8). All animal procedures adhered to the Association for Research in Vision and Ophthalmology Resolution on the Use of Animals in Research.

Physical mapping

YAC clones from the SHR strain were isolated from a commercially available library (Research Genetics, Huntsville, AL) by PCR screening. STSs were generated from YAC insert end sequences isolated by inverse-PCR (51) using *Dpn*II-digested total DNA from YAC-containing clones and primers m and n (T3 side) or o and p (T7 side) (Table 1). STSs derived from chimeric ends were detected by radiation hybrid mapping using a commercially available mapping panel (Research Genetics). BAC

Table 1. Oligonucleotide sequences

a	CATCTGTCCGGAGAGAACTG
b	GTACGACCCATTGTCTGAGC
c	ATCACATCCAGCACACACAG
d	GAACCCAGAAGATGTTGACG
e	GAGCGTGAATGTCACCAGA
f[a]	CTTACTGCAGACCAGCCAAT
g	TTCAGGTCAAGGAAGCTGAC
h[a]	TGAGAATAAACCCGCAGAAG
i	CAACACCGAGTCTATGCTCA
j[a]	ACAGGAAGGTGTGGAGGTCT
k	AGAACTGAGCTCTCAAGGCA
l[a]	CCTCAACACAGAGAAGGTGG
m	GTAAATTAACCCTCACTAAAGGGAATTC
n	CGATGATAAGCTGTCAAACATGAG
o	TGGGGTAAGTGCACTAGGGT
p	CGTAATAATACGACTCACTATAGGGAATT
BACT7	TAATACGACTCACTATAGGG
BACSp6	CGTCGACATTTAGGTGACACT

[a]Murine sequence.

clones were isolated by hybridization-based screening of the BN-derived RPCI-32 BAC library (BAC PAC Resources, Roswell Park Cancer Institute, Buffalo, NY). Insert end sequences were obtained by cycle sequencing using Big Dye terminators (PE Biosystems) with BACT7 and BACSp6 primers (Table 1) on Qiagen (Valencia, CA) Tip-500-purified BAC DNA. BAC inserts were sized by pulsed-field gel electrophoresis, and STSs were generated from insert end sequences as previously described (28).

Dissection of retinal tissues

Neural retina was isolated from RPE/scleral tissue of P22–P28 rats. The cornea of an enucleated eye bathed in phosphate-buffered saline (PBS; calcium and magnesium free) was pierced with a no. 11 scalpel blade, and the cornea and iris were removed using a forceps and iris scissors. While keeping the eye in the buffer, the retina was isolated from RPE/sclera by holding the sclera near the optic nerve head with a curved Dumont forceps, while gently squeezing and pushing towards the corneal window with another forceps. The lens and vitreous were removed from the isolated retina.

Expression analysis

Poly(A) RNA samples (2.5 µg) were electrophoresed in a 1.2% agarose–formaldehyde gel and blotted onto a nylon membrane (Millipore, Bedford, MA). A 537 bp antisense DNA probe (Fig. 2c) was labeled with ^{32}P by linear amplification and hybridized to the membrane in a formamide-based solution at 42°C. The membrane was washed with 1× SSC, 0.1% SDS at 65°C. A rat multiple tissue northern blot (Clontech, Palo Alto, CA) was hybridized following the manufacturer's protocol. For RT–PCR, 5 µg of total RNA was used for first strand cDNA synthesis with Superscript II (Life Technologies, Gaithersburg, MD), and 1 µl of a 20 µl reaction was used in a 10 µl PCR and analyzed on a 3% agarose gel.

ACKNOWLEDGEMENTS

We thank Dr Gregory Barsh for discussions and comments on the manuscript, and Dr Lubert Stryer for his support. Supported by grants to D.V. from the March of Dimes Birth Defects Foundation and Ruth and Milton Steinbach Fund, and to M.M.L. from the NIH, the Foundation Fighting Blindness and Research to Prevent Blindness.

REFERENCES

1. Young, R.W. and Bok, D. (1969) Participation of the retinal pigment epithelium in the rod outer segment renewal process. *J. Cell Biol.*, **42**, 392–403.
2. Anderson, R.E. and Maude, M.B. (1972) Lipids of ocular tissues VIII: the effects of essential fatty acid deficiency on the phospholipids of the photoreceptor membranes of rat retina. *Arch. Biochem. Biophys.*, **151**, 270–276.
3. Bourne, M.C. and Gruneberg, H. (1939) Degeneration of the retina and cataract, a new recessive gene in the rat. *J. Hered.*, **30**, 130–136.
4. Bourne, M.C., Campbell, D.A. and Tansley, K. (1938) Hereditary degeneration of the rat retina. *Br. J. Ophthalmol.*, **22**, 613–622.
5. Dowling, J.E. and Sidman, R.L. (1962) Inherited retinal dystrophy in the rat. *J. Cell Biol.*, **14**, 73–109.
6. Herron, W.L., Riegel, B.W., Myers, O.E. and Rubin, M.L. (1969) Retinal dystrophy in the rat—a pigment epithelial disease. *Invest. Ophthalmol.*, **8**, 595–604.
7. Bok, D. and Hall, M.O. (1971) The role of the retinal pigment epithelium in the etiology of inherited retinal dystrophy in the rat. *J. Cell Biol.*, **49**, 664–682.
8. LaVail, M.M. and Battelle, B.A. (1975) Influence of eye pigmentation and light deprivation on inherited retinal dystrophy in the rat. *Exp. Eye Res.*, **21**, 167–192.
9. Mullen, R.J. and LaVail, M.M. (1976) Inherited retinal dystrophy: primary defect in pigment epithelium determined with experimental rat chimeras. *Science*, **192**, 799–801.
10. Li, L. and Turner, J.E. (1988) Inherited retinal dystrophy in the RCS rat: prevention of photoreceptor degeneration by pigment epithelial cell transplantation. *Exp. Eye Res.*, **47**, 911–917.
11. Edwards, R.B. and Szamier, R.B. (1977) Defective phagocytosis of isolated rod outer segments by RCS rat retinal pigment epithelium in culture. *Science*, **197**, 1001–1003.
12. McLaughlin, B.J., Cooper, N. and Shepherd, V.L. (1994) How good is the evidence to suggest that phagocytosis of ROS by RPE is receptor mediated? *Prog. Retin. Eye Res.*, **1**, 147–164.
13. Mayerson, P.L. and Hall, M.O. (1986) Rat retinal pigment epithelial cells show specificity of phagocytosis *in vitro*. *J. Cell Biol.*, **103**, 299–308.
14. Custer, N.V. and Bok, D. (1975) Pigment epithelium–photoreceptor interactions in the normal and dystrophic rat retina. *Exp. Eye Res.*, **21**, 153–166.
15. Gery, I. and O'Brien, P.J. (1981) RCS rat macrophages exhibit normal ROS phagocytosis. *Invest. Ophthalmol. Vis. Sci.*, **20**, 675–679.
16. Finnemann, S.C., Bonilha, V.L., Marmorstein, A.D. and Rodriguez-Boulan, E. (1997) Phagocytosis of rod outer segments by retinal pigment epithelial cells requires alpha(v)beta5 integrin for binding but not for internalization. *Proc. Natl Acad. Sci. USA*, **94**, 12932–12937.
17. Boyle, D., Tien, L.F., Cooper, N.G., Shepherd, V. and McLaughlin, B.J. (1991) A mannose receptor is involved in retinal phagocytosis. *Invest. Ophthalmol. Vis. Sci.*, **32**, 1464–1470.
18. Sparrow, J.R., Ryeom, S.W., Abumrad, N.A., Ibrahimi, A. and Silverstein, R.L. (1997) CD36 expression is altered in retinal pigment epithelial cells of the RCS rat. *Exp. Eye Res.*, **64**, 45–56.
19. Cai, L., Schalkwyk, L.C., Schoeberlein-Stehli, A., Zee, R.Y., Smith, A., Haaf, T., Georges, M., Lehrach, H. and Lindpaintner, K. (1997) Construction and characterization of a 10-genome equivalent yeast artificial chromosome library for the laboratory rat, *Rattus norvegicus*. *Genomics*, **39**, 385–392.
20. Haldi, M.L., Lim, P., Kaphingst, K., Akella, U., Whang, J. and Lander, E.S. (1997) Construction of a large-insert yeast artificial chromosome library of the rat genome. *Mamm. Genome*, **8**, 284.
21. Brown, D.M., Matise, T.C., Koike, G., Simon, J.S., Winer, E.S., Zangen, S., McLaughlin, M.G., Shiozawa, M., Atkinson, O.S., Hudson Jr, J.R. *et al.* (1998) An integrated genetic linkage map of the laboratory rat. *Mamm. Genome*, **7**, 521–530.
22. Watanabe, T.K., Bihoreau, M.T., McCarthy, L.C., Kiguwa, S.L., Hishigaki, H., Tsuji, A., Browne, J., Yamasaki, Y., Mizoguchi-Miyakita, A., Oga, K.

et al. (1999) A radiation hybrid map of the rat genome containing 5,255 markers. *Nature Genet.*, **22**, 27–36.
23. Steen, R.G., Kwitek-Black, A.E., Glenn, C., Gullings-Handley, J., Van Etten, W., Atkinson, O.S., Appel, D., Twigger, S., Muir, M., Mull, T. *et al*. (1999) A high-density integrated genetic linkage and radiation hybrid map of the laboratory rat. *Genome Res.*, **9**, AP1–AP8.
24. LaVail, M.M. (1981) Assignment of retinal dystrophy (*rdy*) to linkage group IV of the rat. *J. Hered.*, **72**, 294–296.
25. Jacob, H.J., Brown, D.M., Bunker, R.K., Daly, V.J., Dzau, V.J., Goodman, A., Koike, G., Kren, V., Kurtz, T., Lander, E.S. *et al*. (1995) A genetic linkage map of the laboratory rat, *Rattus norvegicus*. *Nature Genet.*, **9**, 63–69.
26. LaVail, M.M. (1981) Photoreceptor characteristics in congenic strains of RCS rats. *Invest. Ophthalmol. Vis. Sci.*, **20**, 671–675.
27. Canzian, F. (1997) Phylogenetics of the laboratory rat *Rattus norvegicus*. *Genome Res.*, **7**, 262–267.
28. Vollrath, D. and Jaramillo-Babb, V.L. (1999) A sequence-ready BAC clone contig of a 2.2 Mb segment of human chromosome 1q24. *Genome Res.*, **9**, 150–157.
29. Graham, D.K., Dawson T.L., Mullaney, D.L., Snodgrass, H.R. and Earp, H.S. (1994) Cloning and mRNA expression analysis of a novel human protooncogene, c-mer. *Cell Growth Differ.*, **5**, 647–657.
30. Crosier, K.E. and Crosier, P.S. (1997) New insights into the control of cell growth; the role of the Axl family. *Pathology*, **29**, 131–135.
31. Graham, D.K., Bowman, G.W., Dawson, T.L., Stanford, W.L., Earp, H.S. and Snodgrass, H.R. (1995) Cloning and developmental expression analysis of the murine c-mer tyrosine kinase. *Oncogene*, **10**, 2349–2359.
32. Camenisch, T.D., Koller, B.H., Earp, H.S. and Matsushima, G.K. (1999) A novel receptor tyrosine kinase, Mer, inhibits TNF-alpha production and lipopolysaccharide-induced endotoxic shock. *J. Immunol.*, **162**, 3498–3503.
33. McCloskey, P., Fridell, Y., Attar, E., Villa, J., Jin, Y., Varnum, B. and Liu, T. (1997) GAS6 mediates adhesion of cells expressing the receptor tyrosine kinase Axl. *J. Biol. Chem.*, **272**, 23285–23291.
34. Anderson, D.H., Johnson, L.V. and Hageman, G.S. (1995) Vitronectin receptor expression and distribution at the photoreceptor–retinal pigment epithelial interface. *J. Comp. Neurol.*, **360**, 1–16.
35. Vuori, K. and Ruoslahti, E. (1994) Association of insulin receptor substrate-1 with integrins. *Science*, **266**, 1576–1578.
36. Klemke, R.L., Yebra, M., Bayna, E.M. and Cheresh, D.A. (1994) Receptor tyrosine kinase signaling required for integrin alpha v beta 5-directed cell motility but not adhesion on vitronectin. *J. Cell Biol.*, **127**, 859–866.
37. Allen, L.A. and Aderem, A. (1996) Mechanisms of phagocytosis. *Curr. Opin. Immunol.*, **8**, 36–40.
38. Little, C.W., Castillo, B., DiLoreto, D.A., Cox, C., Wyatt, J., del Cerro, C. and del Cerro, M. (1996) Transplantation of human fetal retinal pigment epithelium rescues photoreceptor cells from degeneration in the Royal College of Surgeons rat retina. *Invest. Ophthalmol. Vis. Sci.*, **37**, 204–211.
39. Lu, Q., Gore, M., Zhang, Q., Camenisch, T., Boast, S., Casagranda, F., Lai, C., Skinner, M.K., Klein, R., Matsushima, G.K. *et al*. (1999) Tyro-3 family receptors are essential regulators of mammalian spermatogenesis. *Nature*, **398**, 723–728.
40. Nagata, K., Ohashi, K., Nakano, T., Arita, H., Zong, C., Hanafusa, H. and Mizuno, K. (1996) Identification of the product of growth arrest-specific gene 6 as a common ligand for Axl, Sky and Mer receptor tyrosine kinases. *J. Biol. Chem.*, **271**, 30022–30027.
41. Chen, J., Carey, K. and Godowski, P.J. (1997) Identification of Gas6 as a ligand for Mer, a neural cell adhesion molecule related receptor tyrosine kinase implicated in cellular transformation. *Oncogene*, **14**, 2033–2039.
42. Nakano, T., Ishimoto, Y., Kishino, J., Umeda, M., Inoue, K., Nagata, K., Ohashi, K., Mizuno, K. and Arita, H. (1997) Cell adhesion to phosphatidylserine mediated by a product of growth arrest-specific gene 6. *J. Biol. Chem.*, **272**, 29411–29414.
43. Anderson, R.E. and Maude, M.B. (1970) Phospholipids of bovine outer segments. *Biochemistry*, **9**, 3624.
44. Fadok, V.A., Bratton, D.L., Frasch, S.C., Warner, M.L. and Henson, P.M. (1998) The role of phosphatidylserine in recognition of apoptotic cells by phagocytes. *Cell Death Differ.*, **5**, 551–562.
45. Weier, H.U., Fung, J. and Lersch, R.A. (1999) Assignment of protooncogene *MERTK* (a.k.a. c-mer) to human chromosome 2q14.1 by *in situ* hybridization. *Cytogenet. Cell Genet.*, **84**, 91–92.
46. Gu, S.M., Thompson, D.A., Srikumari, C.R., Lorenz, B., Finckh, U., Nicoletti, A., Murthy, K.R., Rathmann, M., Kumaramanickavel, G., Denton, M.J. and Gal, A. (1997) Mutations in *RPE65* cause autosomal recessive childhood-onset severe retinal dystrophy. *Nature Genet.*, **17**, 194–197.
47. Marlhens, F., Bareil, C., Griffoin, J.-M., Zrenner, E., Amalric, P., Eliaou, C., Liu, S.Y., Harris, E., Redmond, T.M., Arnaud, B. *et al.* (1997) Mutations in *RPE65* cause Leber's congenital amaurosis. *Nature Genet.*, **17**, 139–140.
48. Maw, M.A., Kennedy, B., Knight, A., Bridges, R., Roth, K.E., Mani, E.J., Mukkadan, J.K., Nancarrow, D., Crabb, J.W. and Denton, M.J. (1997) Mutations of the gene encoding cellular retinaldehyde-binding protein in autosomal recessive retinitis pigmentosa. *Nature Genet.*, **17**, 198–200.
49. Petrukhin, K., Koisti, M.J., Bakall, B., Li, W., Xie, G., Marknell, T., Sandgren, O., Forsman, K., Holmgren, G., Andreasson, S. *et al.* (1998) Identification of the gene responsible for Best macular dystrophy. *Nature Genet.*, **19**, 41–47.
50. Laird, P.W., Zijderveld, A., Linders, K., Rudnicki, M.A., Jaenisch, R. and Berns, A. (1991) Simplified DNA isolation procedure. *Nucleic Acids Res.*, **19**, 4293.
51. Silverman, G.A., Ye, R.D., Pollock, K.M., Sadler, J.E. and Korsmeyer, S.J. (1989) Use of yeast artificial chromosome clones for mapping and walking within human chromosome segment 18q21.3. *Proc. Natl Acad. Sci. USA*, **86**, 7485–7489.